Impact of Computational Physics on Multi-scale CFD and Related Numerical Algorithms

R. S. Myong

Department of Mechanical and Aerospace Engineering, Research Center for Aircraft Parts Technology, Gyeongsang National University, Jinju, Gyeongnam 660-701, South Korea

myong@gnu.ac.kr

Abstract: Development of accurate computational methods for the constitutive relation that plays a role as the bridge between microscopic and macroscopic physics becomes a key issue in a continuum approach for describing rarefied and micro-scale gas flows. The mathematical form of the constitutive relation dictates the resulting computational methods and related algorithms. It is, therefore, vital to develop proper computational models on the basis of a correct understanding of the multi-scale physics inherent in non-equilibrium gases. In this study the computational issue is discussed by considering two benchmark multi-scale problems: the compression-dominated shock structure and velocity shear-dominated gas flows. Special emphasis is placed on efficient CFD algorithms within the finite volume formulation. In addition, the verification and validation issue of the multi-scale methods is discussed and a simple verification method based on basic physical laws is proposed.

Keywords: CFD, micro-scale and rarefied gas, constitutive equation, multi-scale method

1 Introduction

The study of the behavior of rarefied and micro-scale gases is not only a fundamentally challenging subject, but also has emerged as a significant technical issue [1-4]. It is generally believed, however, that owing to formidable challenges in theoretical and computational aspects associated with the multi-scale nature of the problem, our understanding of the fundamental physics that lie behind this subject is limited. Also, the computational physics, which concerns the study of computational models for a given physical problem as opposed to the analysis of numerical methods for a given computational model, becomes a key issue during the initial phase

of the study of CFD algorithms for rarefied and micro-scale gases. It is, therefore, vital to first develop proper computational models based on a correct understanding of the multi-scale aspects of gases.

There exist various computational methods [5-16] for the multi-scale modeling of gas flows: the molecular approach, the continuum approach, and the hybrid method. In particular, the continuum approach based on conservation laws, which had been initially considered inadequate for high non-equilibrium gas flows, has been studied actively in recent years. The success of the continuum approach depends on the so-called constitutive relation that represents the relationship between the microscopic and macroscopic physics of a specific substance of interest. It is the only ingredient that appears in the continuum mechanics intended to bridge two distinctive worlds (macroscopic and microscopic). For this reason, the mathematical form of the constitutive relation dictates the resulting computational methods and related algorithms [4]. It is also well-known that the verification and validation of computational models for rarefied and micro-scale gases is extremely difficult due to the lack of experimental data. In particular, flows involving solid surfaces are considered most challenging owing to the complexity associated with the gas-surface molecular interaction.

In this study, these computational issues are discussed by considering two benchmark problems: the compression-dominated shock structure and velocity shear-dominated gas flows, which highlight the essence of rarefied and micro-scale gases. Special emphasis is placed on efficient gas-kinetic theory based computational models and CFD methods to bridge the gap between microscopic and macroscopic theory. As an example, a finite volume formulation based on the nonlinear coupled constitutive relation (hereafter called NCCR [4]) is developed and its applications to benchmark problems are described. Finally, the verification and validation issue of the multi-scale methods is discussed and a simple verification method based on basic physical laws is proposed.

2 Computational methods for the multi-scale gas flows

The approach to develop the computational models can be, in general, classified into three categories: molecular, continuum, and hybrid.

2.1 Molecular approach

This approach is mostly based on the molecular description of gases: namely the Boltzmann

transport equation. For this reason, the approach can provide computational models capable of simulating gas flows in all regimes including the transition and free-molecular regimes. One of the most successful methods in this category is the direct simulation Monte Carlo (DSMC) [5], which has been extensively used for the computation of rarefied gas flows. However, the computational cost is usually very high in comparison with that of the continuum models, in particular, in regimes near the continuum limit. Another important method in this category is the computational method based on the linearized Boltzmann equation [6]: for example, Sone's method [7]. Also, a new class of this approach was developed on the basis of a simplified Boltzmann equation on a discrete lattice, which is known in the literature as the lattice-Boltzmann method (LBM) [8]. It was found that the LBM can handle a high Knudsen number regime and is highly parallelizable owing to the locality of the scheme.

2.2 Continuum approach

All the continuum models are based on the conservation laws of density, momentum, and energy. However, they differ in how to describe the higher order fundamental variables appearing in the conservation laws of momentum and energy: namely, the viscous stress tensor and heat flux vector. The continuum models come under the general category of the Chapman-Enskog method or the moment method. The continuum approach can basically produce continuum hydrodynamic equations such as the Burnett equations [9], the Grad's moment equations [10,11], the generalized hydrodynamic equations [1-4,12], and the regularized moment equations [13]. These continuum models were developed from the kinetic transport equations, with emphasis on computational efficiency. Even though in these models there are questions of validity regimes and of physical consistency, such as the second law of thermodynamics, the models allow analytical solutions to be derived and, by doing so, provide physical intuitions that may not be available in the case of the molecular approach. The continuum models originating from the kinetic theory of gases are illustrated in Fig. 1.

2.3 Hybrid method

It is possible to couple the molecular method with a simplified version of the continuum models, in most cases, the Navier-Stokes-Fourier equations. The hybrid method can be developed for problems that contain disconnected high non-equilibrium domains embedded in continuum gas flows. Since this method takes advantage of the good properties of the continuum and molecular methods, it can provide considerable benefits, in particular, in computational aspects.

Some hybrid methods for micro- and nano-scale gas flow [14] and for hypersonic gas flow [15] have been reported recently. Also, a seamless multi-scale method [16], in which the viscous stress in the macroscopic model is calculated by the molecular dynamics model, has been proposed.

3 Multi-scale CFD algorithm based on nonlinear coupled constitutive relation

3.1 Finite volume formulation

The multi-scale computational model is based on the following conservation laws

$$\frac{\partial}{\partial t}\int_V \mathbf{U}dV + \int_S \mathbf{F}\cdot\mathbf{n}dS = 0\,, \qquad (3.1)$$

where S represents the bounding surface of the control volume V and

$$\mathbf{U} = \begin{bmatrix} \rho \\ \rho\mathbf{u} \\ \rho E_t \end{bmatrix},\ \mathbf{F} = \begin{bmatrix} \rho\mathbf{u} \\ \rho\mathbf{u}\mathbf{u} + p\mathbf{I} \\ (\rho E_t + p)\mathbf{u} \end{bmatrix} + \begin{bmatrix} \mathbf{0} \\ \boldsymbol{\Pi} \\ \boldsymbol{\Pi}\cdot\mathbf{u} + \mathbf{Q} \end{bmatrix}. \qquad (3.2)$$

Here $\rho, \mathbf{u}, p, E_t$ represent the density, the velocity vector, the pressure, and the total energy, respectively. The non-conserved variables $\boldsymbol{\Pi}$ and $\mathbf{Q}$ denote the viscous stress tensor and the heat flux vector, respectively. The discretized form of the conservation laws in the finite volume formulation can be expressed as, in the two-dimensional case,

$$\mathbf{U}_{i,j}^{n+1} = \mathbf{U}_{i,j}^{n} - \frac{\Delta t}{A_{i,j}}\sum_{k=1}^{N}\mathbf{R}_k^{-1}\mathbf{F}_k^n\Delta L_k\,, \qquad (3.3)$$

where $\mathbf{U}_{i,j}$ is the cell-averaged variable, $\mathbf{F}_k$ is the numerical flux through the cell interface, $A_{i,j}$ is the cell area, ΔL_k is the interface length, and N is the number of interfaces in a cell. $\mathbf{R}_k$ is the rotational matrix and a transformation law of the rotational invariance

$$\boldsymbol{\Pi} = \mathbf{R}^{-1}\tilde{\boldsymbol{\Pi}}\mathbf{R} \qquad (3.4)$$

relates the tensor $\boldsymbol{\Pi}$ in the (x, y) coordinates and the tensor $\tilde{\boldsymbol{\Pi}}$ in the (n, s) coordinates [2]. Notice that the numerical flux is not fully defined until a relationship between the thermodynamic

driving forces and the viscous stress tensor and the heat flux vector is given. For example, when the degree of departure from thermal equilibrium is small, the relationship is reduced to the following Newtonian law of viscosity and the Fourier law of heat conduction

$$\mathbf{\Pi}_{\mathrm{NSF}} = -2\eta\left[\nabla\mathbf{u}\right]^{(2)},\ \mathbf{Q}_{\mathrm{NSF}} = -k\nabla T \qquad (3.5)$$

where η, k represent the viscosity and the thermal conductivity, respectively. Here the symbol $[\ ]^{(2)}$ stands for a traceless symmetric part of the tensor. The pressure p and the temperature T are related by the equation of state. In the case of the NCCR model, the corresponding relationship is expressed in terms of nonlinear coupled functions f_{Π}, f_{Q}, as follows:

$$\mathbf{\Pi} = f_{\Pi}\left(\mathbf{\Pi}_{\mathrm{NSF}}, \mathbf{Q}_{\mathrm{NSF}}, p, T\right),\ \ \mathbf{Q} = f_{Q}\left(\mathbf{\Pi}_{\mathrm{NSF}}, \mathbf{Q}_{\mathrm{NSF}}, p, T\right), \qquad (3.6)$$

which is illustrated in Fig. 2. Note that the multi-scale physics of gases is represented solely by these functions and thus the functions will play a critical role in the computational model and the associated algorithms.

3.2 Iterative solutions of the NCCR model

The nonlinear coupled algebraic constitutive relation can be written in component form [1-4]

$$\begin{bmatrix} 0 \\ 0 \end{bmatrix} = -\begin{bmatrix} 2\left[\mathbf{\Pi}\cdot\nabla\mathbf{u}\right]^{(2)} \\ C_p\mathbf{\Pi}\cdot\nabla T + \mathbf{Q}\cdot\nabla\mathbf{u} \end{bmatrix} - \begin{bmatrix} 0 \\ a\mathbf{I}\cdot\mathbf{\Pi} \end{bmatrix} - p\begin{bmatrix} 2\left[\nabla\mathbf{u}\right]^{(2)} \\ C_p\nabla T \end{bmatrix} + \begin{bmatrix} \mathbf{\Lambda}^{(\Pi)} \\ \mathbf{\Lambda}^{(Q)} \end{bmatrix} \qquad (3.7)$$

where a, C_p represent the uniform force exerted on the gas molecule and the heat capacity per mass at constant pressure, respectively. The dissipation terms on the right-hand side $\mathbf{\Lambda}^{(\Pi,Q)}$ are directly related to the details of the collision integral in the Boltzmann equation. In many cases, for mathematical simplicity, a relaxation approximation for the collision integral is often used and the dissipation term is then reduced to

$$\mathbf{\Lambda}^{(\Pi)} = -\frac{p}{\eta}\mathbf{\Pi},\ \ \mathbf{\Lambda}^{(Q)} = -\frac{pC_p}{k}\mathbf{Q}. \qquad (3.8)$$

On the other hand, in the present NCCR model based on the moment method [12], the dissipation

terms may be expressed as

$$\boldsymbol{\Lambda}^{(\boldsymbol{\Pi})} = -\frac{p}{\eta}\boldsymbol{\Pi} q(\kappa), \quad \boldsymbol{\Lambda}^{(Q)} = -\frac{pC_p}{k}\mathbf{Q} q(\kappa) \qquad (3.9)$$

where

$$q(\kappa) \equiv \frac{\sinh\kappa}{\kappa}, \quad \kappa = \frac{(mk_B T)^{1/4}}{\sqrt{2}pd}\left[\frac{\boldsymbol{\Pi}:\boldsymbol{\Pi}}{2\eta} + \frac{\mathbf{Q}\cdot\mathbf{Q}}{k/T}\right]^{1/2}. \qquad (3.10)$$

In this expression, κ is the first-order cumulant of the cumulant approximation for the dissipation terms; d, m, k_B denote the diameter of the molecule, the molecular mass, and the Boltzmann constant, respectively. Finally, the nonlinear coupled (implicit algebraic) constitutive relation can be written

$$q(\kappa)\begin{bmatrix}\boldsymbol{\Pi}\\ \mathbf{Q}\end{bmatrix} = \begin{bmatrix}-2\eta\left[\nabla\mathbf{u}\right]^{(2)}\\ -k\nabla T\end{bmatrix} + \frac{1}{p}\begin{bmatrix}-2\eta\left[\boldsymbol{\Pi}\cdot\nabla\mathbf{u}\right]^{(2)}\\ -k\boldsymbol{\Pi}\cdot\nabla T - \eta\mathbf{Q}\cdot\nabla\mathbf{u}/\mathrm{Pr}\end{bmatrix} + \frac{1}{p}\begin{bmatrix}0\\ -ka\mathbf{I}\cdot\boldsymbol{\Pi}/C_p\end{bmatrix} \qquad (3.11)$$

In general, the constitutive equation (3.11) consists of nine equations of the viscous stress tensor $\boldsymbol{\Pi}$ and the heat flux vector $\mathbf{Q}$ for the known eleven parameters $(\boldsymbol{\Pi}_{\mathrm{NSF}}, \mathbf{Q}_{\mathrm{NSF}}, p, T)$. Owing to the highly nonlinear terms, it is not obvious whether the constitutive equation can be solved in an efficient way. However, a method based on the concept of the splitting of the velocity vectors into two distinct components, as shown in Fig. 3, can be developed. That is, in the case of a two-dimensional problem, the stress tensor and the heat flux vector components $(\Pi_{xx}, \Pi_{xy}, Q_x)$ on a line in the two-dimensional physical plane induced by thermodynamic forces (u_x, v_x, T_x) can be approximated as the sum of two solvers: (1) one on $(u_x, 0, T_x)$, and (2) another on $(0, v_x, T_x)$.

To illustrate the method, let us consider the solver for the constitutive relation of the one-dimensional compression-expansion case. The resulting equation of normal stress Π divided by the hydrodynamic pressure p is reduced to the following implicit form [1]

$$\hat{\Pi} q(|\hat{\Pi}|) = \hat{\Pi}_0\left(\hat{\Pi}+1\right) \quad \text{where} \quad \hat{\Pi} \equiv \Pi/p,\ q(|\hat{\Pi}|) \equiv \sinh|\hat{\Pi}| \big/ |\hat{\Pi}|, \qquad (3.12)$$

where Π_0 denotes the normal stress described by the Navier-Stokes theory given in (3.5). This implicit equation can be easily solved within a few iterations by the method of iteration, which uses the properties encoded in the equation itself by rearranging it into an equivalent expression of the form

$$\hat{\Pi} = g(\hat{\Pi}) \qquad (3.13)$$

or in expression of the numerical algorithm

$$\hat{\Pi}_{n+1} = g(\hat{\Pi}_n), \quad n = 1, 2, 3, \cdots. \qquad (3.14)$$

The following four functions (I-A, I-B, II, III) may be considered

$$\begin{aligned} &\hat{\Pi}_{n+1} = \sinh^{-1}\left|(1+\hat{\Pi}_n)\hat{\Pi}_0\right|, \quad \hat{\Pi}_{n+1} = -\sinh^{-1}\left|(1+\hat{\Pi}_n)\hat{\Pi}_0\right|, \\ &\hat{\Pi}_{n+1} = \frac{\hat{\Pi}_0}{q(\left|\hat{\Pi}_n\right|) - \hat{\Pi}_0}, \quad \hat{\Pi}_{n+1} = \frac{\hat{\Pi}_n q(\left|\hat{\Pi}_n\right|) - \hat{\Pi}_0}{\hat{\Pi}_0}. \end{aligned} \qquad (3.15)$$

The solutions obtained by these iterative algorithms are depicted in Fig. 4.

3.3 Slip models and issues in the implementation of the algorithm

A simple way to include the velocity slip and temperature jump effect is to make a correction based on the degree of non-equilibrium near the wall surface [17,18].

$$u = \sigma_V l \cdot \Pi_{wall} / \eta \quad \text{and} \quad T = T_{wall} + \sigma_T l \cdot Q_{wall} / k, \quad (3.16)$$

where $l, \sigma_{V,T}$ represent the mean free path, and the slip and jump coefficients, respectively. When the degree of nonequilibrium near the wall surface is taken as linear, the following velocity slip and temperature jump boundary conditions may be derived:

$$u = \sigma_V l \cdot (-)\frac{du}{dy}\Big]_{wall} \quad \text{and} \quad T = T_{wall} + \sigma_T l \cdot (-)\frac{dT}{dy}\Big]_{wall} . \quad (3.17)$$

On the other hand, another model called as the Langmuir slip model [19] has been derived on the basis of the gaseous adsorption isotherm:

$$u = (1-\alpha_V)u_r \quad \text{and} \quad T = \alpha_T T_{wall} + (1-\alpha_T)T_r \quad \text{where} \quad \alpha_{V,T} = \frac{p/p_r}{p/p_r + 4\omega_{V,T}\mathrm{Kn}}. \quad (3.18)$$

Here the subscript *r* denotes a reference value and $\alpha_{V,T}$ represent the fraction of molecules at thermal equilibrium for the velocity and temperature, respectively. The coefficients $\omega_{V,T}$, which are a function of the inverse power law of the gas particle interaction potential and the adsorption potential parameter, play a very similar role to the slip and jump coefficients $\sigma_{V,T}$ in the Maxwell and Smoluchowski models.

The numerical implementation of the present multi-scale computational model, which is comprised of the explicit time integration scheme (3.3) (or equivalent implicit scheme), (3.6), (3.15), (3.16-17) or (3.18), is straightforward, since the structure of the algorithm is exactly the same as that of the Navier-Stokes-Fourier code. Therefore, virtually all the computational methods developed for the Navier-Stokes-Fourier equation can be carried over to the present multi-scale model. For example, the method is easily amenable to parallel processing like domain decomposition method since it retains the locality of the scheme and thus the inter-cell communications remain minimal. As illustrated in Fig. 2, the stress and heat flux at the interface of the cell can be determined locally by the thermodynamic forces defined from two neighboring cells and the algebraic relation NCCR.

3.4 Applications: compression-expansion dominated hypersonic flow and velocity-shear dominated flow

The computational model based on the finite volume formulation given in (3.1)-(3.11), (3.15), and (3.18) has been applied to a realistic problem of technical interests: the compression-expansion dominated hypersonic rarefied gas flows. The presentation of the results published in previous studies [3,20] is repeated here for the purpose of demonstrating the capability of the present multi-scale computational model for compression-expansion dominated hypersonic flow. The shock wave structure of diatomic gases was first computed for various Mach numbers [3]. The results of the inverse density thickness are reproduced in Fig. 5 (a). It can be seen that the NCCR results are in close agreement with the experimental data [21]. The NCCR theory can also be extended to a multi-dimensional case: hypersonic flow with multi-species gases around a reentry vehicle at an altitude of 105 km [20]. Fig. 5 (b) shows normalized temperature contours in the multi-species flowfield around the vehicle for a free-stream Mach number M=23.47. It can be

noticed that the temperature predicted by the NCCR theory is much lower than that of the Navier-Stokes-Fourier theory, in particular, in the wake region.

In order that the NCCR model may be used for gas transport in micro-devices, it must be tested for the velocity shear-dominated gas flow problems. Among various test cases, the compressible Poiseuille gas flow driven by a uniform force [22-25] is first considered due to its simplicity. The force-driven Poiseuille flow is defined as a stationary flow in a slab (or channel) under the action of a constant external force parallel to the walls. It is purely one-dimensional but brings out the essence of the non-classical constitutive relations in states removed from thermal equilibrium. The conservation laws in the case of diatomic gases are reduced to

$$\frac{d}{dy}\begin{bmatrix} \Pi_{xy} \\ p+\Pi_{yy}+\Delta \\ \Pi_{xy}u+Q_y \end{bmatrix} = \begin{bmatrix} \rho a \\ 0 \\ \rho a u \end{bmatrix}. \qquad (3.19)$$

In this expression, the variable Δ denotes the excess normal stress; the corresponding Newtonian law is $\Delta_0 = -\eta_b \nabla \cdot \mathbf{u}$, where η_b denotes the bulk viscosity. The continuum method can differ on how to calculate the fundamental non-conserved variables $\Pi_{xy}, \Delta, \Pi_{yy}, Q_y$ for the given thermodynamic driving forces $\eta u_y, kT_y$. When the conservation laws (3.19) are solved together with the NCCR model (3.11) under the so-called relaxation approximation $q(\kappa) = 1$ and the Langmuir slip model (3.18) [26], it yields temperature profiles that are in qualitative agreement with the DSMC theory, which is demonstrated in Fig. 6.

The Knudsen layer (also known as the kinetic boundary layer) may be defined as the shear flow generated near a wall surface with a channel by the parallel motion of the solid surfaces. Although the Knudsen layer has been investigated extensively in the past using kinetic theory, capturing it within the continuum framework, which may provide distinct advantages in terms of computational efficiency, remains a daunting task [27]. In particular, the exact underlying mechanisms behind the abnormal behaviors in the Knudsen layer (smaller velocity slip and shear stress, nonlinear velocity profile, velocity gradient singularity, non-zero tangential heat flux) are not understood fully. In this study, a phenomenological nonlinear coupled constitutive relation (3.11) with the relaxation approximation is applied to investigate the Knudsen layer problem. The normalized velocity and temperature profiles in the Knudsen layer flow are depicted in Fig. 7. It can be seen that the velocity profile deviates from the linear profile predicted by the Navier-

Stokes-Fourier theory. A similar trend is also found for the case of temperature. In this calculation, the Maxwell and Smoluchowski slip (jump) models are applied. In addition, the NCCR theory predicts smaller velocity slip and larger temperature jump in comparison with the Navier-Stokes-Fourier theory, which is consistent with observations according to the DSMC theory.

4 Verification and validation method for multi-scale models

It is well known that the verification and validation of computational results for rarefied and micro-scale gases is extremely difficult due to the lack of experimental data. In particular, flows involving the solid surface are considered most challenging because the slip boundary conditions make the verification and validation study even harder. However, there can be a self-consistent verification method if one recalls the fact that the conservation laws must be satisfied irrespective of computational models. Furthermore, such a scheme can be easily applied in the case of a pure one-dimensional problem. Here such a verification study on DSMC solutions is conducted by checking the relative internal error of its solutions for the force-driven Poiseuille gas flow studied in the previous section: for example, the x-momentum and the energy equation of the conservation laws (3.19) ($y^* \equiv y/h$),

$$\begin{aligned}
\text{error}_{x\text{-momentum}} &\equiv \frac{T(0)}{\varepsilon_{h_w} T_w} \frac{\Pi_{xy}(y^*)}{p(0)} - \int_0^{y^*} \frac{\rho(y^*)}{\rho(0)} dy^*, \\
\text{error}_{\text{energy}} &\equiv \frac{T(0)}{\varepsilon_{h_w} T_w p(0) u(0)} \left(\Pi_{xy}(y^*) u(y^*) + Q_y(y^*) \right) - \int_0^{y^*} \frac{\rho(y^*)}{\rho(0)} \frac{u(y^*)}{u(0)} dy^*,
\end{aligned} \tag{4.1}$$

where $h, T_w, \varepsilon_{h_w}$ denote the width of a slab, the wall temperature, and a dimensionless number defined as $\varepsilon_{h_w} = ah/RT_w$ in the force-driven Poiseuille gas flow. The x-momentum computational error of the DSMC is plotted in Fig. 8. In the case of NCCR theory, there exists no error owing to the exact approach taken throughout. It can be observed that the relative error of the DSMC increases from the center to the solid wall and reaches a maximum of 1.4% near the wall.

5 Conclusions

The computational physics concerned with developing proper computational models for a

given physical problem plays a dominant role in describing rarefied and micro-scale gases. By considering two benchmark problems, the compression-dominated shock structure and velocity shear-dominated gas flows, the role of computational physics has been illuminated. Special emphasis is placed on efficient CFD algorithms within the finite volume formulation. A simple verification method for multi-scale computational models is also proposed.

Acknowledgements

This work was supported by the Priority Research Centers Program through the National Research Foundation of Korea (NRF), funded by the Ministry of Education, Science and Technology (Grant No. 2010-0029690), and partially by the Degree and Research Center for Aerospace Green Technology (DRC) of the Korea Aerospace Research Institute (KARI), funded by the Korea Research Council of Fundamental Science & Technology (KRCF).

References

[1] Myong, R.S. (1999). Thermodynamically consistent hydrodynamic computational models for high-Knudsen-number flows. *Phys. Fluids* 11(9), 2788-2802.

[2] Myong, R.S. (2001). A computational method for Eu's generalized hydrodynamic equations of rarefied and microscale gasdynamics. *J. Comp. Phys.* 168, 47-72.

[3] Myong, R.S. (2004). A generalized hydrodynamic computational model for rarefied and microscale diatomic gas flows. *J. Comp. Phys*. 195, 655-676.

[4] Myong, R.S. (2009). Coupled nonlinear constitutive models for rarefied and microscale gas flows: Subtle interplay of kinematics and dissipation effects. *Continuum Mech. Thermody.* 21 (5), 389-399.

[5] Bird, G.A. (1994). *Molecular Gas Dynamics and the Direct Simulation of Gas Flows.* Clarendon.

[6] Cercignani, C. (2000). *Rarefied Gas Dynamics: From Basic Concepts to Actual Calculations.* Cambridge.

[7] Sone, Y. (2002). *Kinetic Theory and Fluid Dynamics.* Birkhauser.

[8] Chen, S., and Doolen, G.D. (1998). Lattice Boltzmann method for fluid flows. *Annu. Rev.*

Fluid Mech. 30, 329-364.

[9] Burnett, D. (1935). The distribution of molecular velocities and the mean motion in a nonuniform gas. *Proc. Lond. Math. Soc.* 40, 382-435.

[10] Grad, H. (1949). On the kinetic theory of rarefied gases. *Commun. Pure Appl. Math.* 2, 331-407.

[11] Grad, H. (1952). The profile of a steady plane shock wave. *Commun. Pure Appl. Math.* 5, 257-300.

[12] Eu, B.C. (1992). *Kinetic Theory and Irreversible Thermodynamics.* Wiley.

[13] Torrilhon, M. (2006) Two-dimensional bulk microflow simulations based on regularized Grad's 13-moment equations, *Multiscale Model. Simul.* 5 (3), 695-728.

[14] Nie, X.B., Chen, S.Y., E, W.N., and Robbins, M.O. (2004). A continuum and molecular dynamics hybrid method for micro- and nano-fluid flow. *J. Fluid Mech.* 500, 55-64.

[15] Schwartzentruber, T.E., Scalabrin, L.C., and Boyd, I.D. (2007). A modular particle-continuum numerical method for hypersonic non-equilibrium gas flows. *J. Comp. Phys.* 225, 1159-1174.

[16] Weinan, E., Weiqing, R., and Vanden-Eijnden, E. (2009). A general strategy for designing seamless multiscale methods. *J. Comp. Phys.* 228 (15), 5437-5453.

[17] Maxwell, J.C. (1879). On stresses in rarefied gases arising from inequalities of temperature. *Phil. Trans. Roy. Soc. London.* 170, 231.

[18] von Smoluchowski, M. (1898) Uber den temperauresprung bei warmeleitung in gasen. *Akad. Wiss. Wien*. 107, 304.

[19] Myong, R.S., Lockerby, D.A., Reese, J.M. (2006) The effect of gaseous slip on microscale heat transfer: An extended Graetz problem. *Int. J. Heat Mass Trans.* 49, 2502-2513.

[20] Ahn, J.W. (2010). *Development of multi-species GH equations and analyses of hypersonic rarefied gas flow.* Ph.D. Thesis. Seoul National University.

[21] Alsmyer, H. (1976) Density profiles in argon and nitrogen shock waves measured by the absorption of an electron beam. *J. Fluid Mech.* 74, 497–513.

[22] Uribe, F.J., and Garcia, A.L. (1999). Burnett description for plane Poiseuille flow. *Phys. Rev. E* 60 (4), 4063-4078.

[23] Xu, K. (2003). Super-Burnett solutions for Poiseuille flow. *Phys. Fluids*. 15 (7), 2077-2080.

[24] Xu, K., Liu, H., and Jiang, J. (2007). Multiple temperature kinetic model for continuum and near continuum flows. *Phys. Fluids*. 19, 016101.

[25] Guo, Z.L., and Xu, K. (2009). Numerical validation of Brenner's hydrodynamic model by force driven Poiseuille flow. *Advances in Applied Mathematics and Mechanics*. 1, 391-401.

[26] Myong, R.S. (2011). A full analytical solution for the force-driven compressible Poiseuille gas flow based on a nonlinear coupled constitutive relation. *Phys. Fluids* 23 (1) doi:10.1063/1.3540671.

[27] O'Hare, L., Lockerby, D.A., Reese, J.M., and Emerson, D.R. (2007). Near-wall effects in rarefied gas micro-flows: some modern hydrodynamic approaches. *Int. J. Heat Fluid Flow*. 28 (1), 37-43.

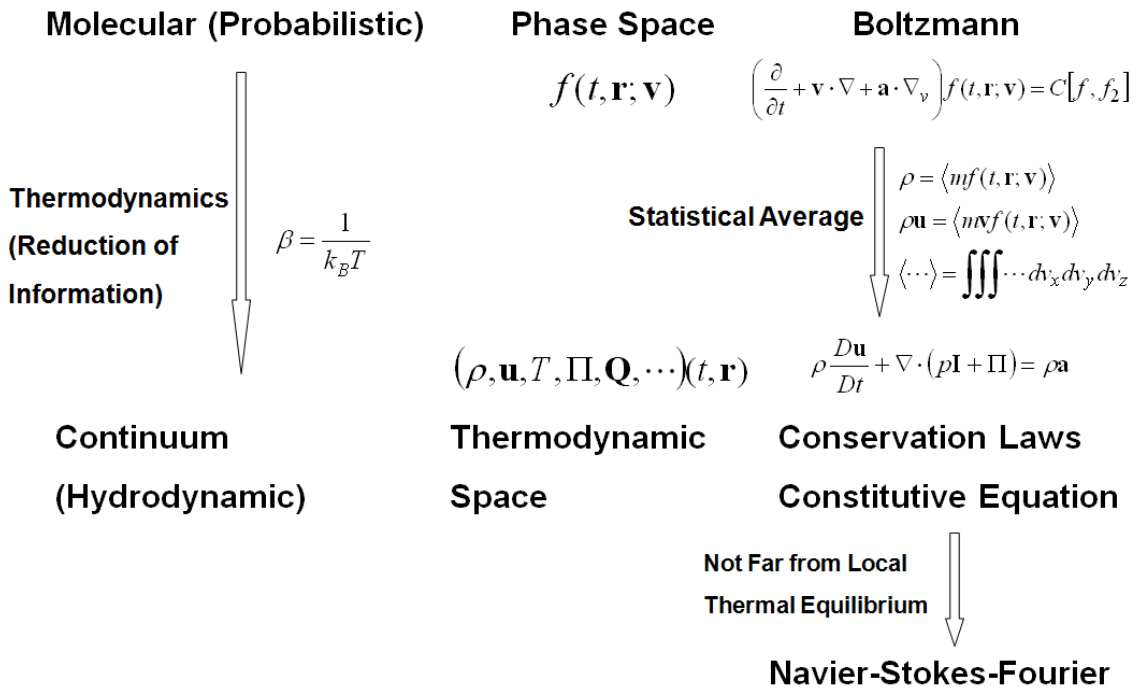

Fig. 1 Relationship between molecular and continuum approaches.

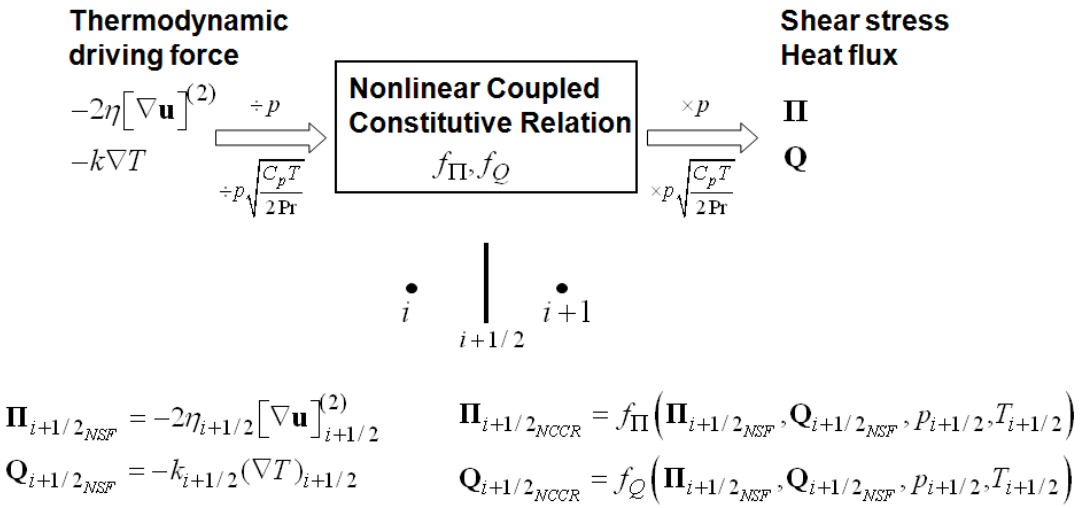

Fig. 2 Relationship between thermodynamic driving forces and the stress tensor and the heat flux vector in the nonlinear coupled constitutive relation.

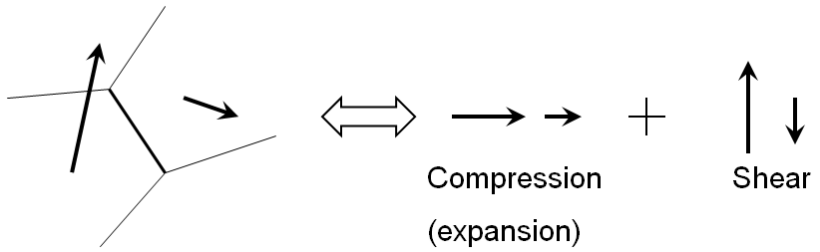

Fig. 3 Splitting of the velocity vectors into two distinct components (compression-expansion and velocity shear flows).

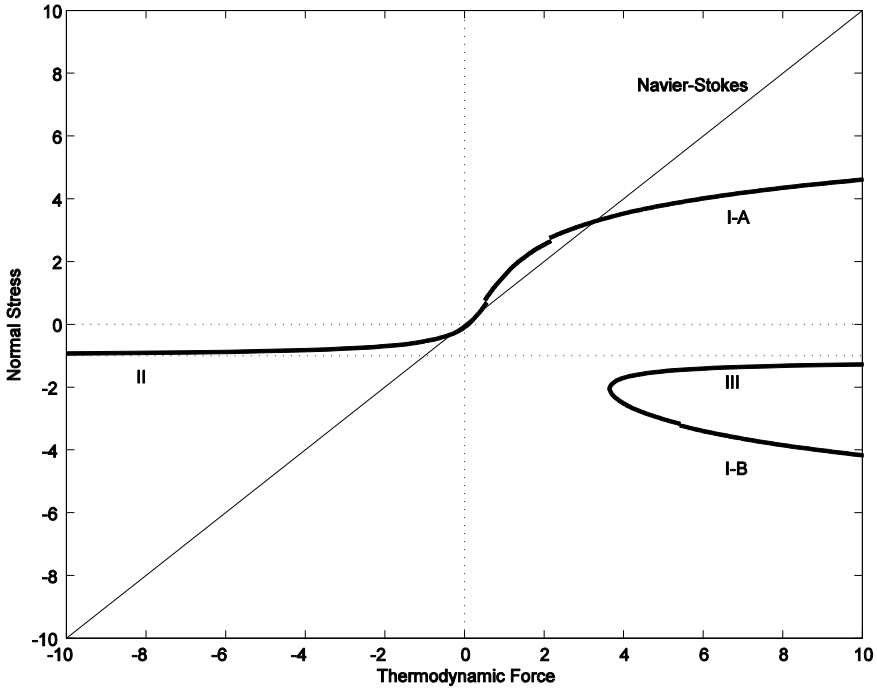

Fig. 4 Iterative solutions of the NCCR model in the case of compression-expansion flow (I-A, I-B, II, III). The horizontal and vertical axes represent the thermodynamic force $\widehat{\Pi}_0$ and the normal stress $\widehat{\Pi}$, respectively. The branches I-A and II that bifurcate from the origin are physically valid solutions.

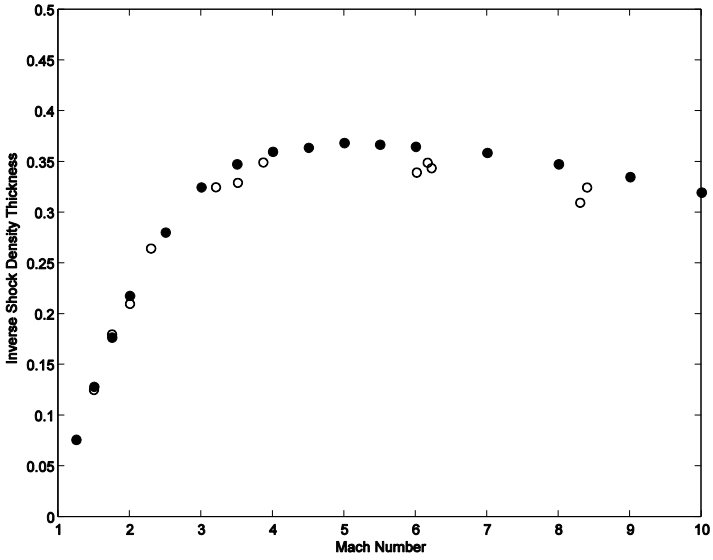

(a)

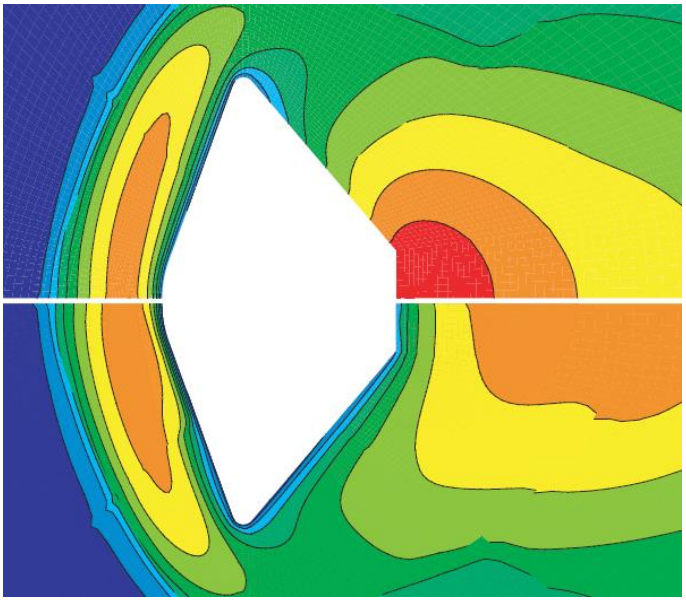

(b)

Fig. 5 (a) Inverse shock density thickness for a diatomic gas (nitrogen) versus the Mach number. The (●) and (○) symbols represent the NCCR theory and the experimental data. (b) Normalized temperature contours in multi-species flowfield around a reentry vehicle (M=23.47, Kn=0.2238, $\omega_{V,T}=1.0$; upper – Navier-Stokes-Fourier, lower – NCCR; red – high temperature, blue – low temperature; courtesy of J. H. Ahn [20]).

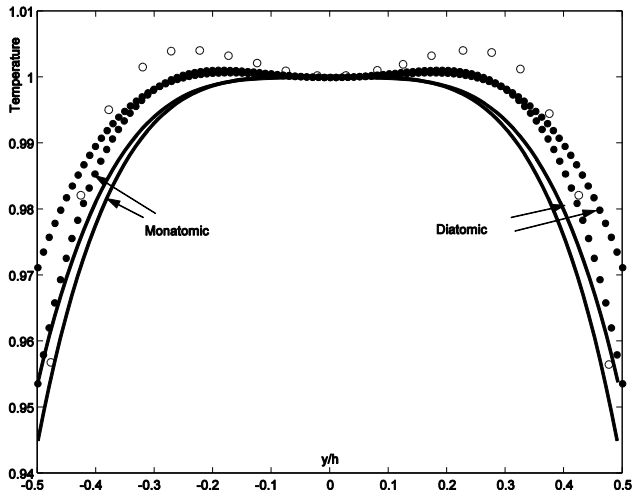

Fig. 6 Temperature distribution across the channel in the compressible Poiseuille gas flow driven by a uniform force (Kn=0.1, ε_{h_w} =0.6, Maxwell gas, $\omega_{V,T}=1.0$, $\eta_b=\eta$). The horizontal axis represents the vertical coordinate in the channel. The (●) and (○) symbols represent the NCCR theory and the DSMC results [22], while the solid lines represent the compressible Navier-Stokes-Fourier results.

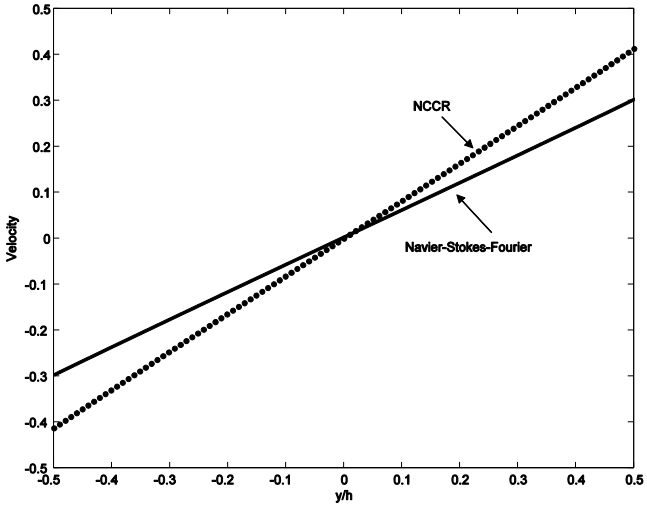

(a)

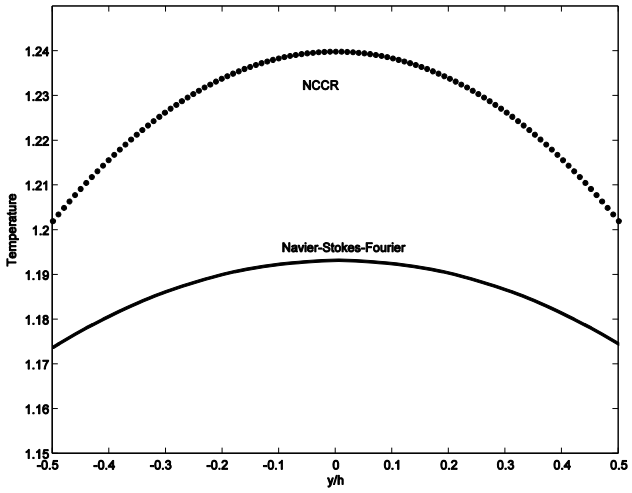

(b)

Fig. 7 Profiles in the Knudsen layer (M=1.0, Kn=1.0, Maxwell gas, $\sigma_V = 1.0$, $\sigma_T = 15/8$):
(a) normalized velocity with respect to the wall velocity, and (b) normalized temperature with respect to the wall temperature. The horizontal axis represents the vertical coordinate in the channel. The (●) symbol and solid lines represent the NCCR theory and the compressible Navier-Stokes-Fourier theory.

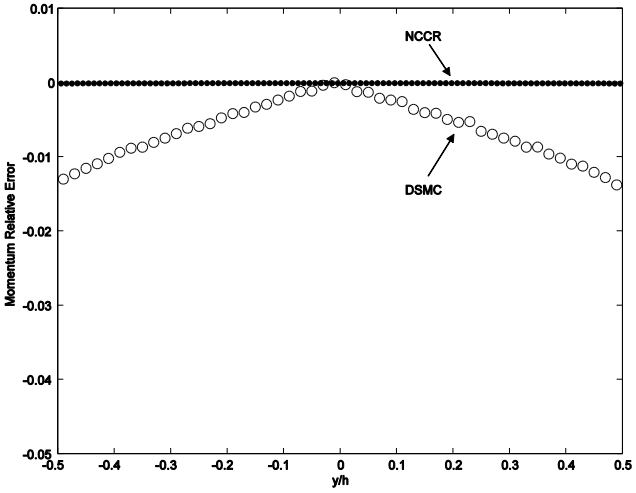

Fig. 8 Distribution of relative computational error in the conservation law of momentum across the channel in the force-driven compressible Poiseuille gas flow (Kn=0.1, ε_{h_w} =0.6, Maxwell gas). The horizontal axis represents the vertical coordinate in the channel. The (●) and (○) symbols represent the NCCR theory and the DSMC result.